

Structural basis for the synthesis of nucleobase modified DNA by *Thermus aquaticus* DNA polymerase

Samra Obeid^a, Anna Baccaro^a, Wolfram Welte^b, Kay Diederichs^b, and Andreas Marx^{a,1}

^aDepartment of Chemistry and ^bDepartment of Biology and Konstanz Research School Chemical Biology, University of Konstanz, Universitätsstrasse 10, D 78457 Konstanz, Germany

Edited by Jack W. Szostak, Massachusetts General Hospital, Boston, MA, and approved October 29, 2010 (received for review September 14, 2010)

Numerous 2'-deoxynucleoside triphosphates (dNTPs) that are functionalized with spacious modifications such as dyes and affinity tags like biotin are substrates for DNA polymerases. They are widely employed in many cutting-edge technologies like advanced DNA sequencing approaches, microarrays, and single molecule techniques. Modifications attached to the nucleobase are accepted by many DNA polymerases, and thus, dNTPs bearing nucleobase modifications are predominantly employed. When pyrimidines are used the modifications are almost exclusively at the C5 position to avoid disturbing of Watson–Crick base pairing ability. However, the detailed molecular mechanism by which C5 modifications are processed by a DNA polymerase is poorly understood. Here, we present the first crystal structures of a DNA polymerase from *Thermus aquaticus* processing two C5 modified substrates that are accepted by the enzyme with different efficiencies. The structures were obtained as ternary complex of the enzyme bound to primer/template duplex with the respective modified dNTP in position poised for catalysis leading to incorporation. Thus, the study provides insights into the incorporation mechanism of the modified nucleotides elucidating how bulky modifications are accepted by the enzyme. The structures show a varied degree of perturbation of the enzyme substrate complexes depending on the nature of the modifications suggesting design principles for future developments of modified substrates for DNA polymerases.

modified nucleotide | nucleobase modification | functional DNA | X-ray structure | PCR

The capability of DNA polymerases to accept modified 2'-deoxynucleoside triphosphates (dNTPs) is exploited in many important biotechnological applications. These include next-generation sequencing approaches (1–3), single molecule sequencing (4), labeling of DNA and PCR amplicates, e.g., for microarray analysis (5–8), DNA conjugation (9), or the in vitro selection of ligands such as aptamers by SELEX (systematic enrichment of ligands by exponential amplification) (10). Furthermore, utilizing the intrinsic properties of DNA in combination with chemically introduced functionalities provides an entry to new classes of nucleic acids-based hybrid materials (9). In most cases the dNTP modifications were introduced to the nucleobase. In cases where pyrimidines are employed the modifications are almost exclusively at the C5 position to avoid disturbing of Watson–Crick base pairing ability (11–20). In addition, the C5 modification is well accommodated into the major groove of DNA without perturbing the DNA structure. Mainly C5 alkyne modified dNTPs are used because they are accessible via metal mediated cross coupling reactions (21–23) in a straightforward manner. While many C5 modified dNTP analogs are already applied, because they are processed by DNA polymerases at least to some extent, it is still unpredictable which modification will be accepted (8, 11–23) because the detailed molecular mechanism by which C5 modifications are accepted by a DNA polymerase is not at all understood. This is largely due to the absence of suitable structural data.

Here, we present unique crystal structures of a DNA polymerase caught while processing two different C5 modified dNTPs, respectively. The large fragment of *Thermus aquaticus* (*Taq*)

DNA polymerase (in short *KlenTaq*, N-terminally truncated form of *Taq* polymerase) was chosen as the target because this enzyme class is heavily employed and well characterized on a functional and structural level (24–31). We compared two dNTP analogs—namely dT^{spin}TP and dT^{dend}TP (Fig. 1A). It was already shown that these nucleotides are able to replace natural dTTP in DNA polymerase-catalyzed reactions (22, 23). In the case of dT^{spin}TP, the nitroxide modification is attached to the C5 position of the nucleobase via a rigid and short acetylene linker that is to ensure direct monitoring of DNA dynamics by EPR (electron paramagnetic resonance) spectroscopy. The dendron-modified substrate dT^{dend}TP is a flexible and sterically demanding modification. The branched architecture that is connected to the nucleobase via a propargylamide linker is considered to explore the size limits of modifications tolerated by DNA polymerases and to introduce multiple functional groups in a single incorporation step. In this study we employed these analogs as models for C5 modified dNTPs because their structure resembles those dNTPs used for other purposes.

Results

Single Nucleotide Incorporation of C5 Modified dNTPs. To investigate the acceptance of the modified nucleotides by *KlenTaq* primer extension studies of single nucleotide incorporation opposite a templating dA was conducted with dTTP and the two modified thymidine analogs in a time-dependent manner. The reaction products of the modified dT^RTP migrate slower than the elongated primer in the presence of dTTP in denaturing polyacrylamide gel electrophoresis (PAGE) due to the additional bulk of the modification (Fig. 1B). Similar effects have been reported before (17, 22, 23). Interestingly, these experiments (Fig. 1B) show the preferential incorporation of the sterically more demanding dT^{dend}TP compared to dT^{spin}TP. The competition experiment, which is performed in presence of the two modified triphosphates with an increasing ratio of dT^{spin}TP, shows more obviously that *KlenTaq* favors dT^{dend}TP over dT^{spin}TP (Fig. 1C).

Quantification of these findings by pre-steady-state kinetics confirmed that indeed dT^{dend}TP is about 20 times more efficiently (k_{pol}/K_D) incorporated compared to dT^{spin}TP (Table 1 and Figs. S1 and S2). Interestingly, the smaller dT^{spin}TP shows higher binding affinity (apparent K_D) to the enzyme as compared to dT^{dend}TP, whereas its incorporation rate (k_{pol}) is significantly more impaired.

Author contributions: S.O. and A.M. designed research; S.O. performed research; S.O. and A.B. contributed new reagents/analytic tools; S.O., W.W., K.D., and A.M. analyzed data; and S.O., K.D., and A.M. wrote the paper.

The authors declare no conflict of interest.

This article is a PNAS Direct Submission.

Data deposition: The atomic coordinates and structure factors have been deposited in the Protein Data Bank, www.pdb.org (PDB ID codes 3OJU and 3OJS).

¹To whom correspondence should be addressed: E-mail: andreas.marx@uni-konstanz.de.

This article contains supporting information online at www.pnas.org/lookup/suppl/doi:10.1073/pnas.1013804107/-DCSupplemental.

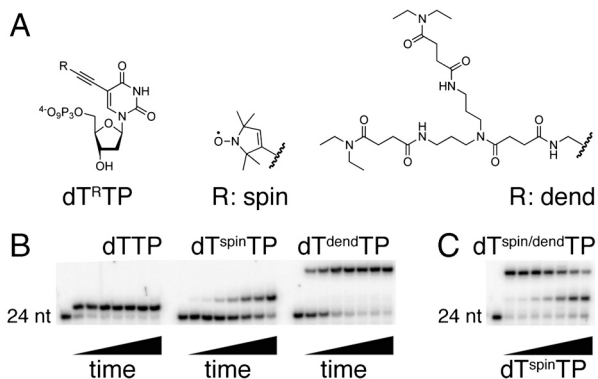


Fig. 1. Comparison of $dT^{\text{spin}}\text{TP}$ and $dT^{\text{dend}}\text{TP}$ in single incorporation experiments. (A) Chemical structure of $dT^{\text{spin}}\text{TP}$ and $dT^{\text{dend}}\text{TP}$. (B) Single nucleotide incorporation of dT^{RTP} for 5, 10, 30, 60, 120, 180, or 300 sec, respectively, using *KlenTaq*. The respective dT^{RTP} is indicated. In each case, the first lane shows the labeled primer. (C) Competition experiment: single nucleotide incorporation in presence of $dT^{\text{spin}}\text{TP}$ and $dT^{\text{dend}}\text{TP}$. The ratio of $dT^{\text{spin}}\text{TP}/dT^{\text{dend}}\text{TP}$ was varied from 1/1 to 100/1 (1/1, 2/1, 4/1, 10/1, 20/1, 50/1, 100/1). The first lane shows the labeled primer.

Structure of *KlenTaq* in Complex with DNA and C5 Modified dNTP. To reveal the structural basis for the ability of DNA polymerases to process an artificial substrate we crystallized *KlenTaq* as ternary complex bound to a primer/template duplex and a respective C5 modified triphosphate in the incoming position. The crystals were obtained by a strategy previously used for *KlenTaq* bound to unmodified substrates (24–26, 28). By incorporation of ddCMP at the primer terminus a primer/template duplex lacking a 3'-terminal hydroxyl group is formed to terminate the primer extension reaction. The structures were solved by difference Fourier techniques and provide snapshots of incorporation of C5 alkyne modified triphosphates at resolutions of 1.9–2.0 Å (Table S1).

Structure of *KlenTaq* in Complex with DNA and $dT^{\text{spin}}\text{TP}$. *KlenTaq* in complex with spin-labeled triphosphate $dT^{\text{spin}}\text{TP}$ (henceforth termed *KlenTaq*_{spin}) adopted an overall conformation very similar to the one in a ternary complex of the enzyme bound to DNA and ddTTP (PDB ID: 1QTM, henceforth termed *KlenTaq*_{1QTM}) described earlier (rmsd for C α 0.392 Å, Fig. S3A and Fig. S4). In *KlenTaq*_{1QTM} ddTTP was bound to the active site due to the applied crystallization strategy (24–26, 28). A zoom into the active site shows that the $dT^{\text{spin}}\text{TP}$ is located opposite to adenine of the template strand, forming Watson–Crick base pairing interactions to the templating base (Fig. 2A) and undergoes π stacking interactions to the 3'-terminus of the primer strand (Fig. S5). The distance from the primer 3'-terminus to the α -phosphate of $dT^{\text{spin}}\text{TP}$ is slightly larger (0.5 Å) than the one in *KlenTaq*_{1QTM} (Fig. 2C). Furthermore, the O helix of the finger domain packs against the nascent base pair forming an active and closed complex similar as with ddTTP. However, Arg660, located at the N terminus of the O helix, shows a different orientation than in *KlenTaq*_{1QTM} and is positioned in a way to make room for the nitroxide modification (Fig. 2). Arg660 has been suggested to stabilize the closed and active conformation via hydrogen-bonding interaction to the phosphate backbone of the primer

Table 1. Transient kinetic parameters for nucleotide incorporation by *KlenTaq* wild type

dT^{RTP}	K_D [μM]	k_{pol} [s^{-1}]	k_{pol}/K_D [$\text{M}^{-1}\text{s}^{-1}$]	Rel. eff. [†]
dTTP	25.0 \pm 3.1	8.80 \pm 0.34	352000	1
$dT^{\text{spin}}\text{TP}$	174 \pm 18	0.02*	132	1/2500
$dT^{\text{dend}}\text{TP}$	381 \pm 30	0.98 \pm 0.03	2572	1/137

*The s.d. in multiple experiments were below significance.

[†]Rel. eff.: relative efficiency; efficiency: k_{pol}/K_D .

3'-terminus (26, 28). This interaction is exclusively observed in the closed conformation and may act as a clamp between the finger domain and the bound DNA duplex (26, 28). The interaction of Arg660 with the primer 3'-terminus is hindered by the rigid nitroxide modification connected to the nucleobase and thereby prevents the stabilization of the closed conformation. As a result of the loss of the hydrogen-bonding interaction, Arg660 shows a high flexibility (B-factor of the amino acid side chain is 81 Å²), and the O helix is slightly shifted (Fig. S6). The missing clamp, between the finger domain and the primer/template duplex, may account for the observed 2,500-fold decrease in incorporation efficiency of $dT^{\text{spin}}\text{TP}$ compared with the natural dTTP.

Structure of *KlenTaq* in Complex with DNA and $dT^{\text{dend}}\text{TP}$. The structure of *KlenTaq* in complex with primer/template duplex and dendron-modified triphosphate $dT^{\text{dend}}\text{TP}$ (henceforth termed *KlenTaq*_{dend}) was determined with a resolution of 1.9 Å. In comparison with *KlenTaq*_{1QTM} the overall conformation of *KlenTaq*_{dend} is very similar, resulting in a low rmsd for C α 0.250 Å (Fig. 4 and Fig. S3B). The $dT^{\text{dend}}\text{TP}$ is captured in the active site waiting for insertion (Fig. 3A). We observe a closed and active complex very similar to *KlenTaq*_{1QTM} and *KlenTaq*_{spin} (Fig. 3B). The same stabilizing factors that are described above such as Watson–Crick base pairing and π stacking interaction are observed (Fig. S5). Even the distance from the primer 3'-terminus to the α -phosphate of the $dT^{\text{dend}}\text{TP}$ is similar to the observed distance in *KlenTaq*_{1QTM} (Fig. 3C). Only partial electron density could be observed for the dendron structure due to the high flexibility of the entity (Fig. 3D and Fig. S4). The rigid propargylamide linkage is well defined, whereas the two flexible branches of the dendron are located outside the active site (Fig. 4). To some extent, one branch reaches in the major groove of the primer/template duplex, indicated by some electron density in this region. The zoom into the active site shows that the finger domain by the O helix packs against the nascent base pair, resulting in a complex poised for catalysis (Fig. S7). Interestingly, in this case the amino acid Arg660 interacts with the phosphate-backbone of the primer 3'-terminus as well as with amide functionality of the propargylamide linkage. Although the described interaction pattern may stabilize Arg660, we observe a high B-factor of the amino acid side chain 97 Å², indicating that the position of Arg660 is tenuous. The geometric freedom of Arg660 may explain the 137-fold reduced incorporation efficiency of $dT^{\text{dend}}\text{TP}$ compared to natural dTTP. In addition, the propargylamide linkage is interacting with the phosphate backbone of the primer 3'-terminus via hydrogen-bonding interactions (Fig. 3). Furthermore, we observe a second hydrogen bond formed between the carbonyl group of an amide in the dendron moiety and the nucleobase of the primer 3'-terminus (Fig. 3D). These hydrogen-bonding interactions might support a nucleotide position and conformation better suited for incorporation compared to $dT^{\text{spin}}\text{TP}$ and more similar to dTTP.

Discussion

Hitherto, structural data of DNA polymerases processing C5 modified pyrimidines that could serve as a guide for structure design of suitable nucleotide modifications was lacking. We present two crystal structures of *KlenTaq* processing differently modified nucleotide analogs. The protein structures in *KlenTaq*_{spin} and *KlenTaq*_{dend} exhibit the incoming nucleotide in a position poised for catalysis similar to the structures reported for *KlenTaq* bound to primer/template and a nucleotide with natural nucleobase (26, 28). Only subtle differences in terms of alignment of the incoming nucleotides, magnesium ions, and water molecules are observed (Fig. S7). This suggests that the enzyme follows similar mechanisms to promote catalysis. However, the structures mainly differ in the position of amino acid side chain Arg660. In *KlenTaq*_{spin} the modified $dT^{\text{spin}}\text{TP}$ obviates Arg660 to undergo

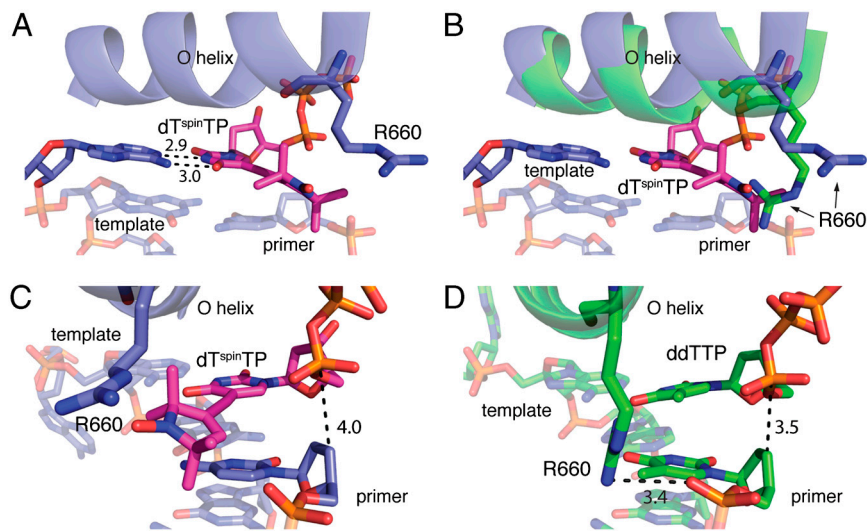


Fig. 2. Structure of *KlenTaq* in complex with $dT^{\text{spin}}\text{TP}$ (*KlenTaq*_{spin}). (A) The close-up view of *KlenTaq*_{spin} (blue) shows the incoming $dT^{\text{spin}}\text{TP}$ (magenta), the O helix with amino acid side chain R660, the primer and template strand. The dashed line highlights the Watson–Crick base pairing interactions. (B) Superimposition of *KlenTaq*_{spin} and *KlenTaq* (green, PDB: 1QTM) highlights the different orientation of the amino acid side chain R660. (C) The distance (shown in dashed lines) of the α -phosphate to the primer 3'-terminus is indicated for *KlenTaq*_{spin}. (D) The distance of the α -phosphate to the primer 3'-terminus (dashed line; 3.5 Å) and the interaction of R660 with the phosphate backbone of the primer 3'-terminus is indicated in dashed line (3.4 Å) for *KlenTaq*. No such interaction is found in *KlenTaq*_{spin} (see C) due to displacement of R660 by the modification.

stabilizing interactions with the primer. In contrast, hydrogen-bonding interactions of the enzyme with $dT^{\text{dend}}\text{TP}$ via the amide functionality of the propargylamide linker are observed in *KlenTaq*_{dend}. The propargylamide linkage as present in $dT^{\text{dend}}\text{TP}$ offers the opportunity to stabilize the closed complex poised for catalysis, which may have beneficial effects on the incorporation efficiency. Amino acid sequence alignment of several DNA polymerases that belong to the same sequence family as *KlenTaq* (i.e., A-family) discloses that the respective arginine is within motif B (32) and is conserved in bacteria (Fig. S8). Thus, it is likely that the depicted mechanism to stabilize the enzyme/substrate complex applies to other DNA polymerases in this sequence family as well.

The results suggest that the modifications are better tolerated by a DNA polymerase if they are attached via linkers that have hydrogen-bonding capability with the enzyme at the depicted positions. In fact, several examples of dNTPs that are processed by DNA polymerases and modified via a C5 propargylamide linker have been reported (1–3, 5, 6, 8, 10–14, 16, 17, 21, 23). These insights suggest that implementing of functionalities with hydrogen binding capability at the discussed position in modified dNTPs may improve their substrate properties. These design guidelines for the development of new modified dNTPs, in combination with directed evolution of DNA polymerases (33–35), will spur the development of future applications.

Materials and Methods

Adducted Protein, Nucleotides, and Oligonucleotides. Protein expression and purification were conducted as described (25–28, 30, 31). Modified thymidine-5'-triphosphates $dT^R\text{TPs}$ were synthesized as described previously. Unmodified dNTPs are commercially available (Roche).

DNA oligonucleotides for enzyme kinetics were synthesized on an Applied-Biosystems 392 DNA/RNA synthesizer and purified by reversed phase HPLC (DMT-ON) and afterwards by preparative PAGE on a 12% polyacrylamide gel containing 8 M urea (DMT-OFF). DNA primer oligonucleotides were labeled with [γ - ^{32}P] ATP using T4 polynucleotide kinase (Fermentas) according to the procedure recommended by the manufacturer.

Single Nucleotide Incorporation Assay. Incorporation opposite dA: 15 μl of the *KlenTaq* reactions contained 50 nM primer (5'-GTG GTG CGA AAT TTC TGA CAG ACA), 75 nM template (5'-GTG CGT CTG TCA TGT CTG TCA GAA ATT TCG CAC CAC), 200 μM dNTPs in buffer (20 mM Tris HCl pH 7.5, 50 mM NaCl, and 2 mM MgCl_2) and 200 nM of *KlenTaq* polymerase. Reaction mixtures were incubated at 37 °C. Incubation times are provided in the respective figure legends. Primer was labeled using [γ - ^{32}P] ATP according to standard techniques. Reactions were stopped by addition of 45 μl stop solution (80% [v/v] formamide, 20 mM EDTA, 0.25% [w/v] bromophenol blue, 0.25% [w/v] xylene cyanol) and analyzed by 12% denaturing PAGE. Visualization was performed by phosphorimaging.

Pre-Steady-State Enzyme Kinetics. The rate of single turnover, single nucleotide incorporation was determined using rapid quench flow kinetics on a chemical quench flow apparatus (RQF-3, KinTek Corp.) as previously described

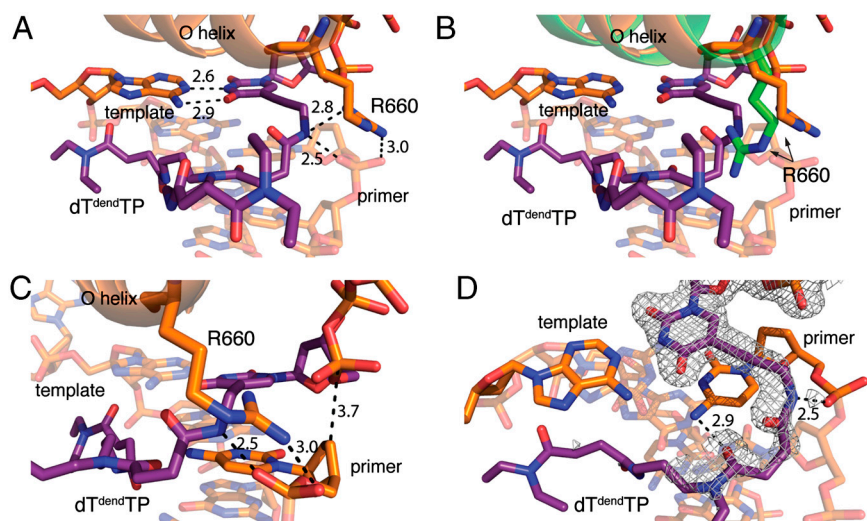


Fig. 3. Structure of *KlenTaq* in complex with $dT^{\text{dend}}\text{TP}$ (*KlenTaq*_{dend}). (A) The close-up view of *KlenTaq*_{dend} (orange) shows the incoming $dT^{\text{dend}}\text{TP}$ (purple), the O helix with amino acid side chain R660, the primer and template strand. The interaction network is indicated in dashed lines as well as the Watson–Crick base pairing interaction between $dT^{\text{dend}}\text{TP}$ and adenine of the template strand. R660 is orientated to allow interaction with the primer 3'-terminus. The amine group of the propargylamide-linkage shows an additional interaction to the primer 3'-terminus. (B) Superimposition of *KlenTaq*_{dend} and *KlenTaq* (green, PDB: 1QTM) highlights the different orientation of the amino acid side chain R660. (C) The interaction pattern of the phosphate backbone at the primer 3'-terminus with R660 and the propargylamide linkage is shown in dashed lines. The distance of the α -phosphate to the primer 3'-terminus is 3.7 Å (highlighted in dashed lines). (D) Interaction network of $dT^{\text{dend}}\text{TP}$ with the primer 3'-terminus toward the phosphate backbone and the nucleobase is indicated with dashed lines. The final refined model map 2mFo-DFc at 1σ is shown for $dT^{\text{dend}}\text{TP}$.

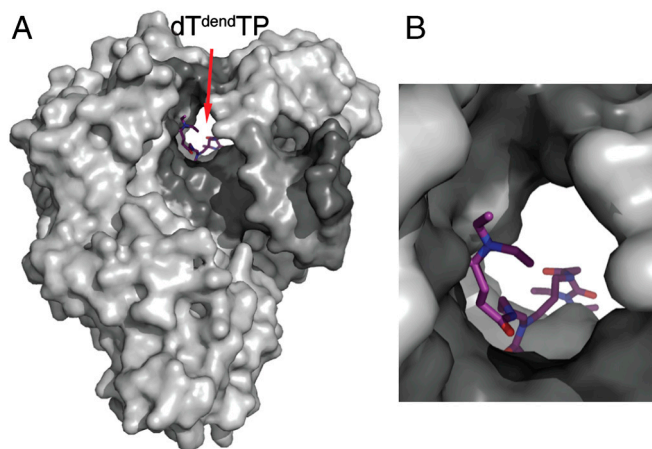


Fig. 4. Structure of *KlenTaq*_{dend} ternary complex. (A) The overall structure of *KlenTaq*_{dend} and the Connolly surface is shown. The incoming dT^{dend}TP is highlighted in sticks and indicated with a red arrow. (B) The close-up view of the incoming dT^{dend}TP illustrates that the dendrimer structure is placed in a left between the protein and primer/template duplex.

(36). For reaction times longer than 5 s manual quenching was performed. In brief, 15 μ l of radiolabelled primer/template complex (50 nM) and DNA polymerase (500 nM) in reaction buffer (RQF buffer, Tris HCl pH 7.5 20 mM, NaCl 50 mM, MgCl₂ 2 mM) (29) were rapidly mixed with 15 μ l of a dNTP solution in reaction buffer at 37 °C. Quenching was achieved by 0.3M EDTA solution (pH 7.0) at defined time intervals. For the investigation of dT^{dend}TP incorporation a 24 nt primer (5'-GTG GTG CGA AAT TTC TGA CAG ACA) and a 36 nt template (5'-GTG CGT CTG TCA TGT CTG TCA GAA ATT TCG CAC CAC) were applied. Quenched samples were analyzed on a 12% denaturing PAGE followed by phosphor imaging. For kinetic analysis experimental data were fit by nonlinear regression using the program GraphPad Prism 4. The data were fit to a single exponential equation: [conversion] = A*(1-exp(-k_{obs}t)). The observed catalytic rates (k_{obs}) were then plotted against the dNTP concentration used and the data were fitted to a hyperbolic equation [k_{obs}] = k_{cat}*[dNTP]/(K_D + [dNTP]) to determine the apparent K_D and k_{cat} of the incoming nucleotide. The incorporation efficiency is given by k_{pol}/K_D. The depicted data derived from double repeated experiments.

- Bentley DR, et al. (2008) Accurate whole human genome sequencing using reversible terminator chemistry. *Nature* 456:53–59.
- Bowers J, et al. (2009) Virtual terminator nucleotides for next-generation DNA sequencing. *Nat Methods* 6:593–595.
- Ruparel H, et al. (2005) Design and synthesis of a 3'-O-allyl photocleavable fluorescent nucleotide as a reversible terminator for DNA sequencing by synthesis. *Proc Natl Acad Sci USA* 102:5932–5937.
- Harris TD, et al. (2008) Single-molecule DNA sequencing of a viral genome. *Science* 320:106–109.
- Guo J, et al. (2008) Four-color DNA sequencing with 3-O-modified nucleotide reversible terminators and chemically cleavable fluorescent dideoxynucleotides. *Proc Natl Acad Sci USA* 105:9145–9150.
- Pollack JR, et al. (1999) Genome-wide analysis of DNA copy-number changes using cDNA microarrays. *Nat Genet* 23:41–46.
- Perou CM, et al. (2000) Molecular portraits of human breast tumours. *Nature* 406:747–752.
- Seo TS, et al. (2005) Four-color DNA sequencing by synthesis on a chip using photocleavable fluorescent nucleotides. *Proc Natl Acad Sci USA* 102:5926–5931.
- Weisbrod SH, Marx A (2007) A nucleoside triphosphate for site-specific labelling of DNA by the Staudinger ligation. *Chem Commun* 18:1828–1830.
- Mayer G (2009) The chemical biology of aptamers. *Angew Chem Int Edit* 48:2672–2689.
- Thum O, Jäger S, Famulok M (2001) Functionalized DNA: A new replicable biopolymer. *Angew Chem Int Edit* 40:3990–3993.
- Weizman H, Tor Y (2002) Redox-active metal-containing nucleotides: Synthesis, tunability, and enzymatic incorporation into DNA. *J Am Chem Soc* 124:1568–1569.
- Giller G, et al. (2003) Incorporation of reporter molecule-labeled nucleotides by DNA polymerases. I. Chemical synthesis of various reporter group-labeled 2'-deoxyribonucleoside-5'-triphosphates. *Nucleic Acids Res* 31:2630–2635.
- Jäger S, Famulok M (2004) Generation and enzymatic amplification of high-density functionalized DNA double strands. *Angew Chem Int Edit* 43:3337–3340.
- Anderson JP, Angerer B, Loeb LA (2005) Incorporation of reporter-labeled nucleotides by DNA polymerases. *Biotechniques* 38:257–264.
- Ohbayashi T, et al. (2005) Expansion of repertoire of modified DNAs prepared by PCR using KOD Dash DNA polymerase. *Org Biomol Chem* 3:2463–2468.

Crystallization and Structure Determination. The closed ternary complexes of *KlenTaq* were obtained by incubating *KlenTaq* in presence of DNA primer (5'-d(GAC CAC GGC GC)-3'), template (5'-d(AAA AGG CGC CGT GGT C)-3'), ddCTP and one of the 5-modified dT^{dend}TP. Thereby, one ddCMP is incorporated, while the corresponding 5-modified dT^{dend}TP is captured in the position waiting for insertion.

*KlenTaq*_{spin}: The crystallization was set up using purified *KlenTaq* (11 mg/ml; buffer: 20 mM Tris HCl pH 7.5, 150 mM NaCl, 1 mM EDTA, 1 mM β -mercaptoethanol), DNA template/primer duplex, ddCTP and dT^{spin}TP in a molar ratio of 1:3:10:20 and in presence of 20 mM MgCl₂. The crystallization solution was mixed in 1:1 ratio with the reservoir solution 0.05 M Tris HCl, pH 9, 0.2 M NH₄Cl, 0.01 M CaCl₂, and 26% PEG 4000.

*KlenTaq*_{dend}: The crystallization was set up using purified *KlenTaq* (11 mg/ml; buffer: 20 mM Tris HCl pH 7.5, 150 mM NaCl, 1 mM EDTA, 1 mM β -mercaptoethanol), DNA template/primer duplex, ddCTP and dT^{dend}TP in a molar ratio of 1:3:10:20 and in presence of 20 mM MgCl₂. The crystallization solution was mixed in 1:1 ratio with the reservoir solution containing 0.05 M sodium cacodylate (pH 6.5), 0.2 M NH₄OAc, 0.01 M Mg(OAc)₂, and 26% PEG 8000.

Crystals were produced by the hanging drop vapor diffusion method, equilibrating against 1 ml of the reservoir solution for 5 d at 18 °C. They were frozen in liquid nitrogen and kept at 100 K during data collection. Data were measured at the beamline PXIII (X06DA) at the Swiss Light Source of the Paul Scherrer Institute (PSI) in Villigen, Switzerland, at a wavelength 1.000 Å and using a Mar225 CCD detector. Data reduction was performed with the XDS package (37, 38). The structures were solved by difference Fourier techniques using *KlenTaq* wild type (PDB 1QTM) as model. Refinement was performed with PHENIX (39) and model rebuilding was done with COOT (40). The structures were refined to a resolution of 2.0 Å in *KlenTaq*_{spin} and 1.9 Å in *KlenTaq*_{dend}. Both structures were in the same space group P3₁21, with cell dimensions a, b 109.0 Å, c 91.5 Å for *KlenTaq*_{spin}, and a, b 107.8 Å, c 90.2 Å for *KlenTaq*_{dend}, respectively. Figures were made with PyMOL (41). The Ramachandran statistics for *KlenTaq*_{spin} show that 91.5% of the residues are in the most favored regions, 7.9% in additional allowed regions, 0.4% in generously allowed and 0.2% in disallowed regions as defined PROCHECK (42). For *KlenTaq*_{dend} the values are 92.3%, 7.5%, 0%, and 0.2%, respectively.

ACKNOWLEDGMENTS. This work was partly funded by the German Excellence Initiative.

- Jäger S, et al. (2005) A versatile toolbox for variable DNA functionalization at high density. *J Am Chem Soc* 127:15071–15082.
- Srivatsan SG, Tor Y (2007) Fluorescent pyrimidine ribonucleotide: Synthesis, enzymatic incorporation, and utilization. *J Am Chem Soc* 129:2044–2053.
- Čapek P, et al. (2007) An efficient method for the construction of functionalized DNA bearing amino acid groups through cross-coupling reactions of nucleoside triphosphates followed by primer extension or PCR. *Chem-Eur J* 13:6196–6203.
- Gramlich PME, Wirges CT, Manetto A, Carell T (2008) Postsynthetic DNA modification through the copper-catalyzed azide-alkyne cycloaddition reaction. *Angew Chem Int Edit* 47:8350–8358.
- Hocek M, Fojta M (2008) Cross-coupling reactions of nucleoside triphosphates followed by polymerase incorporation. Construction and applications of base-functionalized nucleic acids. *Org Biomol Chem* 6:2233–2241.
- Obeid S, Yulikov M, Jeschke G, Marx A (2008) Enzymatic synthesis of multi spin-labeled DNA. *Angew Chem Int Edit* 47:6782–6785.
- Baccaro A, Marx A (2010) Enzymatic synthesis of organic polymer-grafted DNA. *Chem-Eur J* 16:218–226.
- Korolev S, Nayal M, Barnes WM, Di Cera E, Waksman G (1995) Crystal structure of the large fragment of *Thermus aquaticus* DNA polymerase I at 2.5-Å resolution: Structural basis for thermostability. *Proc Natl Acad Sci USA* 92:9264–9268.
- Li Y, Korolev S, Waksman G (1998) Crystal structures of open and closed forms of binary and ternary complexes of the large fragment of *Thermus aquaticus* DNA polymerase I: structural basis for nucleotide incorporation. *EMBO J* 17:7514–7525.
- Li Y, Kong Y, Korolev S, Waksman G (1998) Crystal structures of the Klenow fragment of *Thermus aquaticus* DNA polymerase I complexed with deoxyribonucleoside triphosphates. *Protein* 7:1116–1123.
- Li Y, Mitaxov V, Waksman G (1999) Structure-based design of Taq DNA polymerases with improved properties of dideoxynucleotide incorporation. *Proc Natl Acad Sci USA* 96:9491–9496.
- Li Y, Waksman G (2001) Crystal structures of a ddATP-, ddTTP-, ddCTP-, and ddGTP-trapped ternary complex of KlenTaq1: Insights into nucleotide incorporation and selectivity. *Protein Sci* 10:1225–1233.
- Rothwell PJ, Mitakov V, Waksman G (2005) Motions of the fingers subdomain of klenTaq1 are fast and not rate limiting: Implications for the molecular basis of fidelity in DNA polymerases. *Mol Cell* 19:345–355.

30. Obeid S, et al. (2010) Replication through an abasic DNA lesion: Structural basis for adenine selectivity. *EMBO J* 29:1738–1747.
31. Betz K, et al. (2010) Structures of DNA polymerases caught processing size-augmented nucleotide probes. *Angew Chem Int Edit* 49:5181–5184.
32. Delarue M, Poch O, Tordo N, Moras D, Argos P (1990) An attempt to unify the structure of polymerases. *Protein Eng* 3:461–467.
33. Ramsay N, et al. (2010) CyDNA: Synthesis and replication of highly Cy-dye substituted DNA by an evolved polymerase. *J Am Chem Soc* 132:5096–5104.
34. Leconte AM, et al. (2010) Directed evolution of DNA polymerases for next-generation sequencing. *Angew Chem Int Ed* 49:5921–5924.
35. Staiger N, Marx A (2010) A DNA polymerase with increased reactivity for ribonucleotides and C5-modified deoxyribonucleotides. *ChemBioChem* 11:1963–1966.
36. Di Pasquale F, et al. (2008) Opposed steric constraints in human DNA polymerase beta and *E. coli* DNA polymerase I. *J Am Chem Soc* 130:10748–10757.
37. Kabsch W (2010) XDS. *Acta Crystallogr D* 66:125–132.
38. Kabsch W (2010) Integration, scaling, space-group assignment and post-refinement. *Acta Crystallogr D* 66:133–144.
39. Adams PD, et al. (2002) PHENIX: Building new software for automated crystallographic structure determination. *Acta Crystallogr D* 58:1948–1954.
40. Emsley P, Cowtan K (2004) Coot: Model-building tools for molecular graphics. *Acta Crystallogr D* 60:2126–2132.
41. DeLano WL (2002) *The PyMOL Molecular Graphics System* (DeLano Scientific, Palo Alto, CA).
42. Laskowski RA, MacArthur MW, Moss DS, Thornton JM (1993) PROCHECK—a program to check the stereochemical quality of protein structures. *J Appl Crystallogr* 26:283–291.